INTERSTELLAR POLARIZATION FROM A MEDIUM WITH CHANGING GRAIN ALIGNMENT

P. G. MARTIN

David Dunlap Observatory, Richmond Hill, Ontario, and Scarborough College, University of Toronto

ABSTRACT

If the direction of grain alignment in the interstellar medium changes along the line of sight to a star, circular polarization can be produced. Models are developed for the polarization from such a medium, as the basis for interpreting existing observations. Emphasis is placed on the numerous relationships between circular polarization, linear polarization, and extinction from which information about the interstellar grains can be derived. Detailed applications are made to both stars and clusters of stars. Some new measurements of circular polarization are reported and observational prospects for the future are evaluated.

Subject headings: interstellar matter — interstellar reddening — open clusters — polarization

I. INTRODUCTION

Several important characteristics of interstellar polarization from a medium in which the direction of grain alignment changes along the line of sight are discussed in order to provide the basis for a more quantitative interpretation of available observations and to suggest new directions for exploration. Such a medium produces interstellar extinction and both linear and circular polarization. Thus for any star the possible range of available information includes the degrees of linear and circular polarization as a function of wavelength, the wavelength dependence of the position angle of linear polarization, and the ratio of polarization to extinction. It is shown how analysis of these observations might lead to a better knowledge of the composition of interstellar grains, the mean grain size, and any changes in these properties along the line of sight.

Furthermore it should be possible to estimate the amount by which the orientation of the alignment changes along the line of sight. Because of electric charges on the grains the interstellar magnetic field should always control the direction of grain alignment, regardless of the actual alignment mechanism (Martin 1971); therefore, ultimately the structure of the galactic magnetic field can be investigated. Additional information might be obtained by combining observations of many stars which are in nearly the same direction in the Galaxy.

Linear polarization of starlight has been known for over two decades. The present state of observations in this area has been reviewed recently, by Serkowski (1973) and Coyne (1973). Although the birefringence which accompanies linear dichroism in the interstellar medium was noted by van de Hulst (1957) some time ago, observations of circular polarization are quite new. Circular polarization of interstellar origin was first detected by Martin, Illing, and Angel (1972) in the direction of the Crab Nebula, following predictions by

Martin (1972) that new information about the grain composition could be obtained.

Serkowski (1962) suggested circular polarization could arise in a medium in which the direction of grain alignment changed along the line of sight, as is discussed here, but until the observations of Kemp (1972) observational accuracy was not quite sufficient. Further successful observations are reported by Kemp and Wolstencroft (1972). An interpretation of these early circular-polarization measurements has been presented by Martin (1973). New observations of the circular polarization of stars with a different polarimeter are described in § V.

II. THEORETICAL CONSIDERATIONS

a) Transfer Equations for the Stokes Parameters

One approach to studying quantitatively the polarizing properties of the aligned grains in the interstellar medium is through an analysis of how the grains affect the four Stokes parameters I, Q, U, and V.

Consider first a thin slice of the interstellar medium, perpendicular to the line of sight. The spinning grains in this slice are uniformly aligned, and can be represented schematically as having an elongated mean profile (in the plane of the slice), as shown in figure 1. The linear extinction coefficients, which we define to be $2\sigma_1$ and $2\sigma_2$ for radiation with electric vector parallel to the principal axes 1 and 2 of the slice, respectively, can be calculated as the averages over the grain size and orientation distributions multiplied by the number density of grains (see § II*b*). Similarly the phase shifts per unit pathlength, ϵ_1 and ϵ_2, can be defined.

In the following $\Delta\sigma = \sigma_1 - \sigma_2$ and $\Delta\epsilon = \epsilon_1 - \epsilon_2$ are used to describe the linear dichroism and linear birefringence, respectively. Since for the interstellar grains usually considered $\Delta\sigma$ is positive at optical wavelengths, the electric vector of the polarized starlight lies
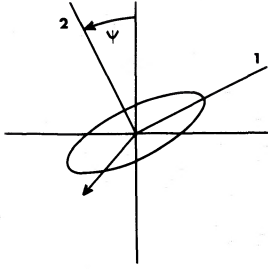
461

Fig. 1.—Schematic representation of the mean grain profile in the plane perpendicular to the line of sight. The direction of propagation of radiation is out of the page, and angle ψ is measured in the sense north through east.

parallel to axis 2 and therefore the angle ψ in figure 1 becomes the polarization position angle. If the sense of grain alignment is as predicted by the Davis-Greenstein mechanism, then axis 2 is the projection of the galactic magnetic field; the only likely alternative is that axis 1 is, since as mentioned above the magnetic field should be an axis of symmetry for any alignment mechanism.

With these definitions we can write down equations for the changes in the Stokes parameters in a slab of thickness ds

$$I^{-1}dI/ds = -(\sigma_1 + \sigma_2), \quad (1)$$

$$d(Q/I)/ds = \Delta\sigma \cos 2\psi, \quad (2)$$

$$d(U/I)/ds = \Delta\sigma \sin 2\psi, \quad (3)$$

$$d(V/I)/ds = \Delta\epsilon(\cos 2\psi U/I - \sin 2\psi Q/I). \quad (4)$$

It is important to note that the first three differential equations are uncoupled, so that integration is greatly simplified. The derivation of these equations, including the approximations involved, is the subject of the Appendix. Here the sign conventions are: positive Q corresponds to position angle zero (usually north); positive U has position angle 45°; for positive V the electric vector rotates counterclockwise, increasing in position angle. It is clear that the interstellar linear polarization arises from the linear dichroism, whereas the circular component depends on several factors: the linear birefringence, the linear polarization present, and some change in ψ along the line of sight. Note that the wavelength dependence of V/I will usually be that of the product $\Delta\epsilon\Delta\sigma$.

b) Calculation of $\Delta\sigma$ and $\Delta\epsilon$

We can interpret the observations of linear and circular polarization using Mie-like calculations for scattering by arbitrarily oriented infinite circular cylinders. As a generalization of the work of Lind and Greenberg (1966) we have defined (Martin 1972) and computed a complex efficiency factor Q; the real part of Q is the extinction efficiency factor, Q_e, whereas the

imaginary part, Q_p, is related to the phase change. These calculations apply as well to cylinders of finite length L and radius a as long as $L \gg a$. We now define the complex cross-section c by

$$c = 2aLQ. \quad (5)$$

If β is the angle between axis 1 of the mean grain profile and the projection of the axis of an individual grain on this plane perpendicular to the line of sight, and if η is the angle between this cylinder axis and the direction of propagation, then following Greenberg (1968)

$$c_1 = c^E(\eta) \cos^2 \beta + c^H(\eta) \sin^2 \beta, \quad (6)$$

$$c_2 = c^E(\eta) \sin^2 \beta + c^H(\eta) \cos^2 \beta, \quad (7)$$

where subscripts 1 and 2 and superscripts E and H identify cross-sections appropriate to radiation with electric vector at position angle 0°, 90°, β, and $\beta + 90°$ relative to axis 1, respectively. These are related to σ and ϵ by (Martin 1972)

$$\sigma_j = 1/2N_g \operatorname{Re} [c_j(\eta)], \quad (8)$$

$$\epsilon_j = 1/2N_g \operatorname{Im} [c_j(\eta)], \quad (9)$$

where N_g is the number density of grains with this orientation.

Suppose that the cylinders are all rotating around short axes aligned at an angle γ to the direction of propagation. The projection of the alignment axis is axis 2 of the mean grain profile. This perfect alignment is a special case; generally the angular velocity will not be parallel to the angular-momentum vector and there will be a distribution of γ centered on the axis of alignment. Now if α is the position angle of the long axis of the grain in the plane perpendicular to the alignment axis, then

$$\Delta\sigma + i\Delta\epsilon = \frac{1}{2}\int_{a_1}^{a_2} N(a)2aL(a)da$$
$$\times \frac{1}{\pi}\int_0^\pi [Q^E(a,\eta) - Q^H(a,\eta)]\cos 2\beta d\alpha, \quad (10)$$

$$\delta = \frac{1}{2}\int_{a_1}^{a_2} N(a)2aL(a)da$$
$$\times \frac{1}{\pi}\int_0^\pi [Q_e^E(a,\eta) + Q_e^H(a,\eta)]d\alpha, \quad (11)$$

where we need the relations

$$\cos \eta = \sin \gamma \cos \alpha, \quad (12)$$

$$\tan \beta = -\cos \gamma \cot \alpha. \quad (13)$$

For the present Q is calculated for infinite cylinders because there is no similar theory for ellipsoidal particles. Equations (10) and (11) are quite general however, should such computations become possible. In the calculations here it has been assumed that L is proportional to a and that $N(a) \propto a \exp\left[-\frac{1}{2}(a/a_0)^2\right]$, both noncritical assumptions.

In figure 2 we have plotted $\Delta\sigma$ and $\Delta\epsilon$ normalized so that $\Delta\sigma(\lambda_{\max}) = 1$, $\lambda_{\max}$ being the wavelength of maximum linear polarization. Curves for two values of the refractive index, $m = 1.5$ and $m = 1.5 - 0.1i$, are shown, calculated with $\gamma = 90°$. In the latter case the size parameter was reduced so that $\lambda_{\max}$ remained the same. The wavelength λ_c at which $\Delta\epsilon$ changes sign is composition dependent. It is seen that for pure dielectric materials the ratio $\lambda_c/\lambda_{\max} \simeq 1$ and that this ratio increases with k, the imaginary part of the refractive index. In fact when k is large, as in metallic materials, there is no crossover in $\Delta\epsilon$ at all. This behavior, described conveniently by changes in $\lambda_c/\lambda_{\max}$, is the basis for studying the grain composition using interstellar polarization observations (Martin 1972).

It should be stressed that this is an effect dependent on absorption by the grain. The real part of the refractive index, n, cannot be obtained from $\lambda_c/\lambda_{\max}$. For instance, if $m = 1.3$, curves similar to the ones for $m = 1.5$ are obtained simply by increasing the size parameter. In fact even k is not determined independently of n; for example, $m = 1.33 - 0.05i$ and $m = 1.5 - 0.1i$ give about equivalent curves. One measure which partly takes into account this dependence of k

on n is the albedo, which stays about the same (0.77 and 0.72, respectively). Clearly the albedo decreases from 1 as $\lambda_c/\lambda_{\max}$ increases.

When $\gamma < 90°$, $\lambda_{\max}$ and λ_c both increase and $\lambda_c/\lambda_{\max}$ remains about the same. Thus the effect on the polarization curves is similar to an increase in n or in the grain size, all scaling the wavelength, but not affecting the shape of the curve much.

The ratio $|\Delta\epsilon/\Delta\sigma|$ for these grains increases away from λ_c. It is never very large for dielectrics, being typically 0.2–0.6 in the near-infrared and blue spectral regions.

c) The Wavelength Dependence of Polarization

The wavelength dependence of linear polarization is not observed to be the same for all stars but recently it has been found that the degree of polarization $P/I(P^2 = Q^2 + U^2)$ plotted on a normalized wavelength scale $\lambda_{\max}/\lambda$, could be approximated analytically for most stars by (Serkowski 1971)

$$(P/I)/(P/I)_{\max} = \exp\left[-1.15 \ln^2\left(\lambda_{\max}/\lambda\right)\right] . \quad (14)$$

There are several factors on which $\lambda_{\max}$ is dependent. For a given grain material $\lambda_{\max}$ increases with the grain size. However the shape of the polarization curve will remain the same only in the special circumstance that the refractive index is independent of wavelength. In addition, when the real part of the refractive index is increased or when the axis of grain alignment is inclined less than 90° to the line of sight, $\lambda_{\max}$ also increases. Thus observations of the variability of $\lambda_{\max}$ have some bearing on studies of grain size and composition in the Galaxy, on the efficiency of the alignment mechanism as a function of grain size, and on the geometry of the alignment.

These shifts in $\lambda_{\max}$ are accompanied by corresponding shifts in λ_c so that the different possible causes are difficult to separate. The alternatives should be kept in mind during the discussion of grain "size" changes in § IV.

d) Geometry-dependent Phenomena

Since $\lambda_{\max}$ is observed to vary from star to star it is not unreasonable to suppose that in some cases $\lambda_{\max}$ also varies along the line of sight. If in addition the direction of the grain alignment also changed, then the position angle of the net polarization would be wavelength dependent (Treanor 1963). As this position-angle dependence has been observed it is important to develop models making quantitative predictions in order to determine whether the above is an acceptable explanation. Equation (14) is adopted for computational convenience in the models below.

Since the degree of linear polarization P/I will usually be measured when V/I is, we may choose to use the relation

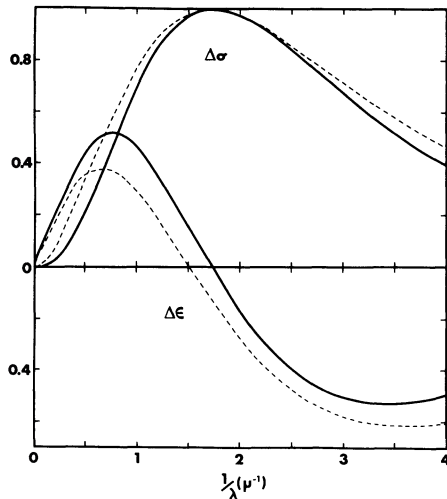$$V/I = (\Delta\epsilon/\Delta\sigma)(P/I)^2 G . \quad (15)$$

Fig. 2.—The linear dichroism $\Delta\sigma$ and linear birefringence $\Delta\epsilon$ for long circular cylinders with refractive indices $m = 1.5$ and $m = 1.5 - 0.1i$ (dashed line). The size parameters were chosen so that the maximum linear polarization occurs at the same wavelength, $\lambda_{\max}$, and the curves are normalized so that $\Delta\sigma(\lambda_{\max}) = 1$.

If $\Delta\epsilon/\Delta\sigma$ is reasonably well-determined from a knowledge of the grain refractive index $(\lambda_c/\lambda_{\max})$, the factor G, indicative of the geometry of the changing alignment, can be estimated. Both $\Delta\epsilon/\Delta\sigma$ and G (§ III) are usually less than 1, so that if P/I is typically 0.01 (1 percent) then $V/I < 10^{-4}$, never very large.

From observations of the degree of linear polarization, p_V (in magnitudes, with the filter of the UBV system) and the color excess, E_{B-V}, for many stars it has usually been found that

$$p_V/E_{B-V} \leq 0.195 . \qquad (16)$$

Some of the causes of why in many cases p_V/E_{B-V} does not attain a high value may be a reduced degree of grain alignment or of elongation of the grain shape, or an unfavourable orientation of the axis of symmetry of the alignment mechanism relative to the line of sight. In addition, if the direction of grain alignment changes along the line of sight the degree of polarization does not build up as much as it would in a more uniform medium. The fact that those regions of the sky where there is a large dispersion in the position angles of polarization usually show low values of p_V/E_{B-V} (e.g., Schmidt 1958) can be taken as evidence for the latter two effects.

We define the depolarization D due to the latter effect by

$$D = (P/I)/(P/I)_0 \leq 1 , \qquad (17)$$

where

$$(P/I)_0 = \int_0^S \Delta\sigma ds . \qquad (18)$$

Clearly a lower limit to D can be estimated from an observation of p_V/E_{B-V} since

$$D \geq (p_V/E_{B-V})/0.195 . \qquad (19)$$

III. MODELS FOR POLARIZATION FROM A MEDIUM WITH CHANGING GRAIN ALIGNMENT

a) Discrete-Slab Models

Our first models are based on finite slabs of the interstellar medium within which it is supposed the alignment is uniform. The ith such slab produces linear polarization $(P/I)_i$ at position angle θ_i; slab 1 is closest to the star being considered. Then according to equations (1)–(4) the net polarization for m slabs, is

$$Q/I = \sum_{i=1}^{m} (P/I)_i \cos 2\theta_i , \qquad (20)$$

$$U/I = \sum_{i=1}^{m} (P/I)_i \sin 2\theta_i , \qquad (21)$$

$$V/I = \sum_{i=2}^{m} \Delta e_i [\cos 2\theta_i \sum_{j=1}^{i-1} (P/I)_j \sin 2\theta_j$$
$$- \sin 2\theta_i \sum_{j=1}^{i-1} (P/I)_j \cos 2\theta_j] , \qquad (22)$$

where

$$\Delta e_i = \int_0^S \Delta\epsilon_i ds . \qquad (23)$$

i) The Two-Slab Model

A simple yet instructive model consists of just two slabs. If the ratio $(P/I)_2/(P/I)_1$ is denoted r, and $\theta_2 - \theta_1 = \phi$, then

$$D^2 = (1 + 2r\cos 2\phi + r^2)/(1 + r)^2 \leq 1 \qquad (24)$$

and

$$V/I = -\Delta e_2 (P/I)_1 \sin 2\phi . \qquad (25)$$

The depolarization D, shown in figure 3, can be considerable. Note that the wavelength dependence of V/I is the product of the wavelength dependences of the birefringence of slab 2 and the dichroism of slab 1. If slab 2 is uniform then

$$G = -r\sin 2\phi/(1 + 2r\cos 2\phi + r^2) . \qquad (26)$$

The function G is plotted in figure 4. It is clear that if the wavelength dependences of linear polarization produced by the two slabs differ, then r, and hence G, will be dependent on wavelength.

Since

$$\tan 2(\theta - \theta_1) = U/Q = r\sin 2\phi/(1 + r\cos 2\phi) , \qquad (27)$$

then θ will also vary with wavelength whenever r does, if $\phi \neq 0$. This formalizes the qualitative interpretation suggested for such observations by Treanor (1963) and Gehrels and Silvester (1965). For quantitative application we note that

$$d\theta/d\lambda = -0.5Gd\ln r/d\lambda . \qquad (28)$$

One axis in figure 4 shows $d\theta/d\ln r$ in degrees.

If r is evaluated on the basis of equation (14), then from equation (28)

$$\lambda_{\max,2}/\lambda_{\max,1} = \exp\left(\frac{-1\lambda}{1.15G}\frac{d\theta}{d\lambda}\right) . \qquad (29)$$
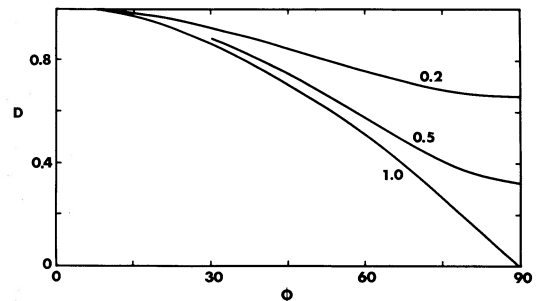

FIG. 3.—The depolarization D of the linear component of polarization due to disorientation ϕ between two successive slabs along the line of sight (eq. [24]). Separate curves are drawn for three different values of r, the ratio of the degrees of linear polarization produced by the two slabs.
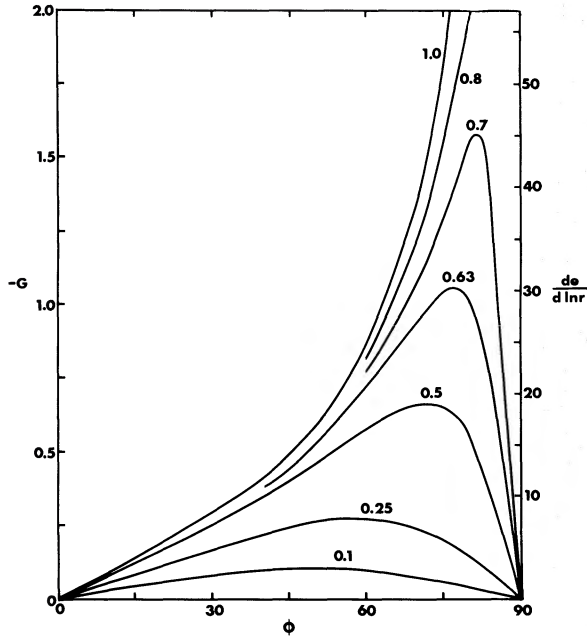
FIG. 4.—The two-slab model for polarization. G is the geometry-dependent factor for circular polarization (eqs. [15] and [26]) and $d\theta/d \ln r$ describes the position-angle change when r is a function of wavelength. Curves are labeled with the corresponding value of r.

Thus measurements of G, from circular-polarization observations, and of $d\theta/d\lambda$ lead simply to an estimate of the change in grain "size" along the line of sight.

ii) The Symmetric Many-Slab Model

In many cases it might be more realistic to consider a model with a large number of slabs. For analysis of linear-polarization observations Serkowski (1962) has considered a related model based on fluctuations in a continuously polarizing medium. Here it is supposed that the polarizing properties $[\theta_i, p_i = (P/I)_i$, and $\Delta e_i]$ of the m slabs are independent, that on the average n slabs are traversed by the line of sight to a star, and that $\theta = 0$ is an axis of symmetry of the position-angle distribution. Then it can be shown from equations (20)–(22) that the *average* values of the Stokes parameters measured for a large number of stars are

$$\langle Q/I \rangle = n \langle p_i \rangle \langle \cos 2\theta_i \rangle , \qquad (30)$$

$$\langle U/I \rangle = \langle V/I \rangle = 0 . \qquad (31)$$

Also

$$\langle (P/I)^2 \rangle = n \langle p_1{}^2 \rangle + (n \langle p_1 \rangle \langle \cos 2\theta_i \rangle)^2 . \qquad (32)$$

The respective dispersions are given by

$$\sigma_{Q/I}{}^2 = n \langle p_i{}^2 \rangle \langle \cos^2 2\theta_i \rangle , \qquad (33)$$

$$\sigma_{U/I}{}^2 = n \langle p_i{}^2 \rangle \langle \sin^2 2\theta_i \rangle , \qquad (34)$$

and

$$\sigma_{V/I}{}^2 = \langle \Delta e_i{}^2 \rangle (n^2 \langle p_i{}^2 \rangle \langle \sin^2 2\theta_i \rangle \langle \cos^2 2\theta_i \rangle$$
$$+ \tfrac{1}{3} n^3 \langle p_i \rangle^2 \langle \sin^2 2\theta_i \rangle \langle \cos 2\theta_i \rangle^2) . \qquad (35)$$

For later convenience we note that from observations of linear polarization we can measure the disorientation of the many slabs using

$$\langle \sin^2 2\theta_i \rangle = \sigma_{U/I}{}^2 / (\sigma_{Q/I}{}^2 + \sigma_{U/I}{}^2) \qquad (36)$$

and predict the dispersion in circular polarization with

$$\sigma_{V/I}{}^2 = \sigma_{U/I}{}^2 (\sigma_{Q/I}{}^2 + \tfrac{1}{3} \langle Q/I \rangle^2)$$
$$\times \langle \Delta e_i{}^2 \rangle / \langle p_i{}^2 \rangle . \qquad (37)$$

Two limiting cases can be discussed, one in which the θ_i are randomly distributed in $0°$–$180°$, and a second in which the θ_i distribution is peaked about $\theta_i = 0$. In the former

$$\langle Q/I \rangle = 0 , \qquad (38)$$

$$\langle (P/I)^2 \rangle = 2\sigma_{Q/I}{}^2 = 2\sigma_{U/I}{}^2 = n \langle p_i{}^2 \rangle , \qquad (39)$$

$$\sigma_{V/I}{}^2 = \langle \Delta e_i{}^2 \rangle / \langle p_i{}^2 \rangle [\tfrac{1}{2} \langle (P/I)^2 \rangle]^2 . \qquad (40)$$

Comparison with equations (17) and (15) suggests that $D \simeq n^{-1/2}$ and $G \simeq 1/2$. Here G is relatively high only because of the large amount of depolarization.

In the peaked distribution, described by Spitzer (1968) for linear-polarization observations,

$$\langle Q/I \rangle = n \langle p_i \rangle , \qquad (41)$$

$$\sigma_{Q/I}{}^2 = n \langle p_i{}^2 \rangle , \qquad (42)$$

$$\sigma_{U/I}{}^2 = n \langle p_i{}^2 \rangle 4 \langle \theta_i{}^2 \rangle , \qquad (43)$$

$$\langle (P/I)^2 \rangle \simeq (n \langle p_i \rangle)^2 , \qquad (44)$$

$$\sigma_{V/I}{}^2 \simeq \langle \Delta e_i{}^2 \rangle / \langle p_i{}^2 \rangle \langle (P/I)^2 \rangle^2 4 \langle \theta_i{}^2 \rangle / 3n . \qquad (45)$$

Therefore $D \simeq 1$ and $G \simeq (4 \langle \theta_i{}^2 \rangle / 3n)^{1/2}$. As expected, when the amount of disorientation is small and the number of slabs is large G (and $\sigma_{V/I}$) are small. In this limit the expected mean square deviation in the observed position angles is found from

$$\sigma_\theta{}^2 = \langle \theta_i{}^2 \rangle / n . \qquad (46)$$

b) Continuous Medium with Uniform Twist

An alternative to the discrete models is one in which the position angle ψ of grain alignment changes monotonically along the line of sight. Kemp and Wolstencroft (1972) have described a model in which $\psi(s) = ks$ ($k = $ constant; $s = 0$ at the star) in an otherwise uniformly polarizing medium, but their analysis applies only in the limit of small ψ. Martin (1973) has

given closed-form solutions, based on integration of equations (2)–(4) with $\psi = ks$. First a straightforward integration of

$$d(Q/I) = \Delta\sigma \cos 2ks \, ds \,, \qquad (47)$$

$$d(U/I) = \Delta\sigma \sin 2ks \, ds \,, \qquad (48)$$

gives

$$Q/I = (\Delta\sigma/2k) \sin 2ks = (P/I)_0 \sin 2\phi/2\phi \,, \qquad (49)$$

$$U/I = (\Delta\sigma/2k)(1 - \cos 2ks) = (P/I)_0(\sin^2 \phi)/\phi \,, \qquad (50)$$

where ϕ is the total twist in the medium traversed. Thus

$$d(V/I) = \Delta\epsilon(\Delta\sigma/2k)(\cos 2ks - 1)ds \,, \qquad (51)$$

from which

$$V/I = -\Delta e(P/I)_0(2\phi - \sin 2\phi)/(2\phi)^2$$

$$= -\Delta e(P/I)_0 v(\phi) \,. \qquad (52)$$

Since

$$P/I = (P/I)_0(\sin \phi)/\phi \qquad (53)$$

it follows that

$$D = (\sin \phi)/\phi \qquad (54)$$

and

$$G = -\tfrac{1}{4}(2\phi - \sin 2\phi)/\sin^2 \phi \,. \qquad (55)$$

The function $v(\phi)$ and D and G are plotted in figure 5. In the limit $\phi \to 0$, $G \simeq -\tfrac{1}{3}\phi$ as derived by Kemp and Wolstencroft (1972). In this limit a regular twist ϕ is equivalent to a rotation $2/3\phi$ in the uniform two slab model. For larger angles a similar ratio holds.
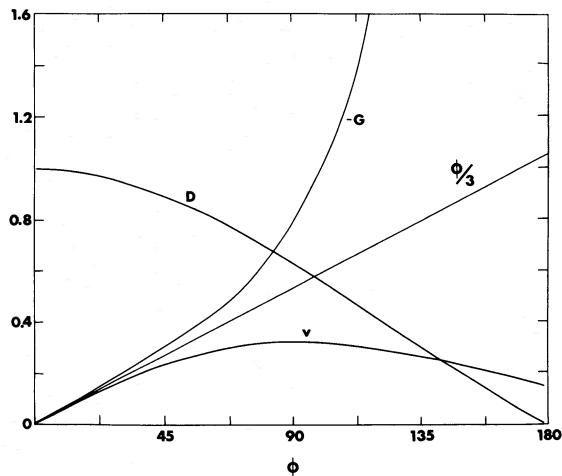

FIG. 5.—Polarization model with uniformly twisting alignment. Curves show the linear depolarization D (eq. [54]) and the geometrical factor G for circular polarization (eq. [55]). Function v (eq. [52]) shows the dependence of circular polarization on the total twist along the line of sight.

The position angle θ of the resulting linear polarization is $1/2\phi$, independent of wavelength. However, wavelength dependence in ϕ can be introduced in the model by allowing the wavelength dependence of $\Delta\sigma$ (and $\Delta\epsilon$) to vary along the line of sight. One simple variation is $\Delta\sigma = \Delta\sigma_0 e^{2r(\lambda)s}$ which together with $\psi = ks$ leads to

$$\tan 2\theta = \frac{(1 - e^{2R} \cos 2\phi) + R/\phi e^{2R} \sin 2\phi}{e^{2R} \sin 2\phi - R/\phi(1 - e^{2R} \cos 2\phi)} \,, \qquad (56)$$

where $R = rs$. The change in θ with R is illustrated by three cases: when $R \to \infty$, $\theta \to \phi$, when $R = 0$, $\theta = 1/2\phi$, and when $R \to -\infty$, $\theta \to 0$. In the limit of small R and small ϕ

$$\theta = \tfrac{1}{2}\phi(1 + \tfrac{1}{6}R) \,, \qquad (57)$$

so that the change in θ can be thought of as a second-order effect.

IV. APPLICATION OF THE MODELS TO OBSERVATIONS

a) Stars

As an example of how the above ideas can be applied to quantitative analysis we consider the two stars σ Sco and o Sco for which both the circular and linear polarization have been measured at a number of wavelengths. Figures 6 and 7 show circular polarization measured by Kemp and Wolstencroft (1972) with the addition of one infrared point for o Sco (see § V). The linear polarization shown is taken from Coyne and Gehrels (1966) and Serkowski (1968), respectively.

i) Grain Composition

The observations displayed here can be used to investigate the grain composition. One striking feature of the observed circular polarization is the sign reversal at visual wavelengths. It is clear from equation (4) that this can be attributed to a sign change of $\Delta\epsilon$, which as pointed out above is a characteristic only of dielectric materials. For highly absorbing materials $\Delta\epsilon$ does not change sign in the range of wavelengths of interest here. In calculating the grain models, we have therefore restricted k to being small.

An attempt has been made to fit the data with simple model grains for which $n = 1.5$ independently of wavelength.[1] For clarity only two values of k, 0 and 0.1, are used here. The size parameter was chosen so that the observed wavelength dependence of linear polarization was reproduced. With this approach the predicted wavelength dependences of circular polarization

---

[1] Since these observations are not a sensitive means of determining n, the choice of $n = 1.5$ is not critical. However, it should be remembered that the ratio $\Delta\sigma/\delta$, a measure of the degree of linear polarization relative to extinction, is systematically higher when n is larger. This becomes important in determining the degree of alignment necessary to explain the observations, a subject we do not deal with here.
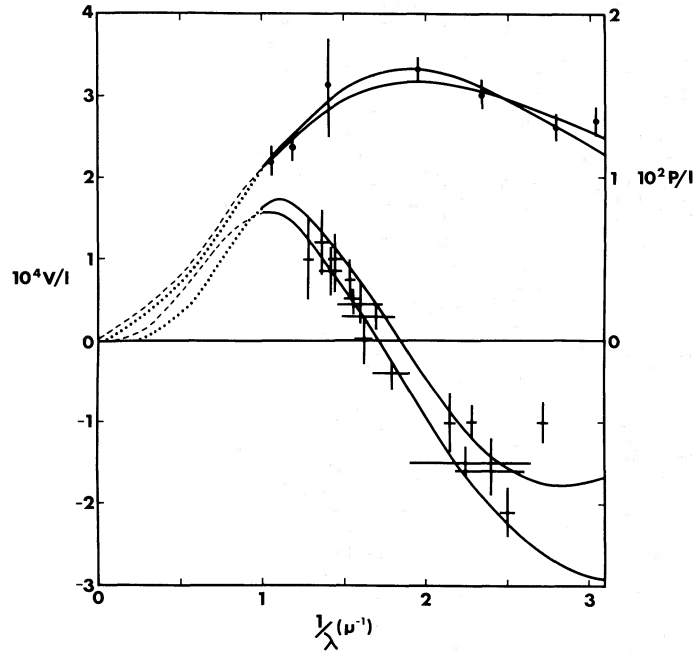
FIG. 6.—Model fitting of linear and circular polarization observations of σ Sco with constant refractive indices $m = 1.5$ (*dotted line*) and $m = 1.5 - 0.1i$ (*dashed line*). Observations are by Coyne and Gehrels (1966) and Kemp and Wolstencroft (1972), respectively. Note the predicted peaks of interstellar circular polarization in the observable spectrum, near 1 and 3 μ^{-1}.

can be used to place limits on k. In addition the scaling required to fit the observations of V/I gives the value of G. (Here it is assumed that G is wavelength independent.)

Considering the simplicity of the present analysis, the computed curves fit both the linear- and circular-polarization observations well, lending support to our assumption that the circular polarization is of interstellar origin. For the polarizing grains a value of k much larger than 0.1 seems unlikely if $n = 1.5$. This is equivalent to concluding that the grains are not so "dirty" as to have an albedo smaller than 0.7.

Similar conclusions about the dielectric nature of the grain material were reached earlier for another direction in the Galaxy, towards the Crab Nebula, from the first interstellar circular-polarization observations (Martin *et al.* 1972). Some other less direct evidence which points toward dielectric materials has been noted by Martin (1973). It is important that circular-polarization observations be extended to other directions in the Galaxy. Preliminary results in a number of different regions (Kemp and Wolstencroft 1972; also § V) indicate that without exception V/I changes sign from red to blue wavelengths as for the stars described above.

ii) *Structure of the Magnetic Field*

Having placed the above restrictions on the type of grain material we now have a reliable measure of G (see table 1). From G we may find how much the alignment
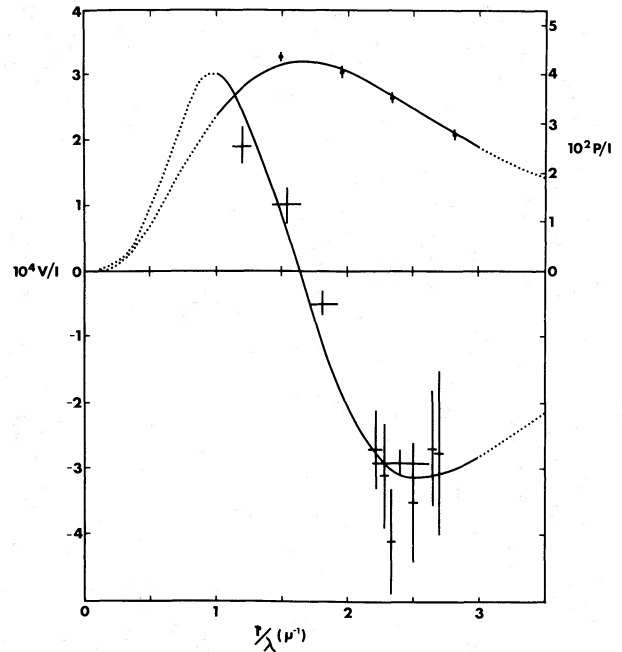

FIG. 7.—Model fitting of linear and circular polarization observations of o Sco by Serkowski (1968) and Kemp and Wolstencroft (1972), respectively. The circular polarization measurement in the near-infrared is from table 3. Only one refractive index, $m = 1.5$, was used.

P. G. MARTIN

TABLE 1

THE CHANGE IN GRAIN ALIGNMENT, ϕ, AS DETERMINED FROM THE OBSERVED
GEOMETRY-DEPENDENT PARAMETERS G AND D, FOR σ AND o SCO

STAR	G AND D	TWIST ϕ	TWO-SLAB MODEL		
			ϕ ($r = 1$)	ϕ ($r = 0.5$)	r (or r^{-1})
σ Sco......	$G = 2$	-120	-76	...	≥ 0.8
	$D \geq 0.46$	≤ 115	≤ 63	≤ 70	≥ 0.37
o Sco......	$G = 0.5$	-70	-46	$-54(-82)$	≥ 0.45
	$D \geq 0.61$	≤ 94	≤ 53	≤ 56	≥ 0.24

changes along the line of sight. According to the model with the uniform twist (fig. 5) $\phi \simeq -120°$ and $-70°$ for σ Sco and o Sco respectively (see table 1). Note that these angles are both within the broad maximum of $v(\phi)$ for which there is optimum circular polarization. A two-slab model requires smaller values of ϕ, about one-third lower if $r = 1$ (fig. 4, table 1); various limits on r (or equivalently on r^{-1}) can be established as indicated in table 1.

Using E_{B-V} from Garrison (1967) and p_V from figures 6 and 7 we find lower limits to $D(\phi)$ for σ Sco and o Sco to be 0.46 and 0.61, respectively. The corresponding upper limits to $|\phi|$ and r (or r^{-1}) are listed in table 1. These limiting values of $|\phi|$ derived from D are reasonably consistent with the angle ϕ required to explain the degree of circular polarization. Together these results suggest that a significant proportion of the "depolarization" for these stars might be attributed to the disorientation in alignment along the line of sight. (One alternative approach to that used here would be to use the upper limits on ϕ from D to establish upper limits on G and hence lower limits to $\Delta\epsilon/\Delta\sigma$.)

We conclude from the present analysis that there is strong evidence for a large change (or large changes) in the direction of grain alignment, and consequently of the direction of the projection of the magnetic field, along the line of sight to these stars. Inspection of the map of electric vectors compiled by Mathewson and Ford (1970) shows that the region we are looking at is a region with a large dispersion in position angles, where fluctuations in the magnetic field are important. The amount of disorientation of the electric vectors in the upper Scorpius region suggests that some version of the many-slab model might be more appropriate, although complete data for a large number of stars are not available. We note that for the other star in this region observed by Kemp and Wolstencroft (1972), ρ Oph, G has the opposite sign, although ρ Oph is about as close to o Sco as σ Sco is. This no doubt reflects the variety of conditions present in different parts of the complex dark clouds.

iii) Grain "Size"

The mean grain size may be defined in a number of ways; for example, as the average weighted according to the contribution to the total extinction. The size determined from fitting the observations also depends

on the refractive index, among other parameters referred to earlier. Here we shall use the term "size" in a more general sense, as it is revealed by λ_{max}.

The wavelength λ_{max} is significantly larger for o Sco than for σ Sco (Carrasco, Strom, and Strom 1973). The value of λ_{max} for σ Sco is about average for all directions in the Galaxy (Serkowski 1973) but the larger wavelength for o Sco is more typical for stars in the Ophiucus cloud complex (Carrasco et al. 1973). Therefore we might conclude that the grain size required to explain the polarization observations is larger for o Sco than for σ Sco.

One way to follow up the hypothesis that a change in grain size is the correct explanation for the observed change in λ_{max} is to study the corresponding effects of such a change on the interstellar extinction curve. Serkowski (1973) has found by plotting the observed extinction on the λ_{max}/λ scale, that the extinction curves for different stars (in particular, stars in Perseus and stars in Scorpius) then agree with one another better than the unscaled ones did. Thus the wavelength shift detected in the polarization observations is apparent in the extinction observations as well. Carrasco et al. (1973) reach similar conclusions for the Ophiucus dark cloud by studying the variations of the ratio of total to selective extinction and the slope of the ultraviolet portion of the extinction curve with λ_{max}. In general good correspondence as in the above cases may not always be found, since all grains causing interstellar extinction need not produce polarization (e.g., spherical grains, composition, or size dependent alignment).

Also one might expect that the wavelength, λ_c, of the crossing point (zero) in the circular polarization would increase with λ_{max}. The observations available for these two stars only hint at this effect (figs. 6 and 7). Actually this is also not a rigid requirement, since λ_{max} depends on an average of $\Delta\sigma$ over the whole path to the star, whereas λ_c is generally more heavily dependent on the part of the medium nearer to the observer; therefore, any changes in the mean grain properties along the line of sight do not necessarily affect λ_{max} and λ_c equally. Smaller foreground grains may explain why for o Sco apparently $\lambda_{max} > \lambda_c$.

iv) Grain "Size" Changes along the Line of Sight

The presence of circular polarization for σ Sco has been interpreted as the result of a change in the direction of grain orientation along the line of sight.

It is therefore interesting that the polarization position angle of σ Sco is wavelength dependent, since this reinforces the interpretation of changing alignment. However, in order that the position angle change it is necessary that λ_{max} (i.e., the wavelength dependence of linear polarization) also change along the line of sight. We analyze the observations of σ Sco according to the two-slab model to see if the above is a reasonable explanation.

Serkowski's (1968) measurements indicate that $\theta_V - \theta_U = -4°3$ and $\theta_V - \theta_B = -2°4$ in the UBV system. A less-certain observation shows this trend continues toward even shorter wavelengths. With $\lambda = 4300$ Å as a representative wavelength, then $\lambda d\theta/d\lambda = -0.21$ radians. Previously we determined that $G \simeq 2$. Then using equation (29) we find that $\lambda_{max,2}/\lambda_{max,1} = 1.1$. This is to be compared to the range of λ_{max} for neighboring stars in upper Scorpius, which is 5550–8100 Å (Carrasco et al. 1973) or a maximum ratio 1.46. We see that the calculated change in λ_{max} along the line of sight to σ Sco is reasonable. If the "size" change in front of o Sco were the same, then the lack of a detectable position angle change could be attributed to the lower value of G or ϕ.

The following detailed picture has emerged from the two-slab model for the polarization of σ Sco. The nearer slab is rotated clockwise by a large angle, about 80°, relative to the other. This causes considerable depolarization of the linear component. At least in the nearer slab the grains are dielectric with an albedo likely to be greater than 0.7; they are slightly "larger" than in the more distant slab. The ratio of the degrees of linear polarization produced by the two slabs is restricted to the range 0.8–1.2.

b) Clusters

An opportunity to use the analysis based on many-slab models arises when the polarization of many stars in a cluster has been observed. No such circular-polarization measurements exist, but we are able to use the available linear-polarization results to make a quantitative prediction of $\sigma_{V/I}$, the expected dispersion in circular polarization for given clusters. This can be used along with other criteria in selecting clusters for which a systematic study of circular polarization would be feasible.

The double cluster h and χ Persei is a good example of a cluster for which the many-slab model is appropriate, but despite the strong linear polarization it is not likely to be a good candidate for circular-polarization studies, since the dispersion in observed position angles is small (4°). The observed linear-polarization parameters are summarized in table 2 (Serkowski 1965, 1968). From equation (36) $\langle \sin^2 2\theta_i \rangle = 0.5$ or roughly $|\theta_i| \simeq 22°5$, which is quite large. However $\sigma_{V/I}/(\langle \Delta e_i^2 \rangle/\langle p_i^2 \rangle)^{1/2} = 9 \times 10^{-5}$, which is small because of the large number of slabs ($n \geq 70$ from eqs. [30] and [33]) along the line of sight (see eq. [45]). The calculated value $\sigma_\theta = 2°7$ (eq. [46]) is reasonably close to the observed 4°, and $D \simeq 1$, suggesting that this model is realistic. If we assume that $(\langle \Delta e^2 \rangle/\langle p_i^2 \rangle)^{1/2} \simeq 0.3$ for dielectric materials, and take into account that the calculation of $\sigma_{V/I}$ above was based on the maximum linear polarization, then $\sigma_{V/I} < 3 \times 10^{-5}$. This seems to be too low to make a search worthwhile, considering the faintness of the cluster stars.

A better opportunity may be provided by the highly reddened cluster VI Cygni, for which the dispersion in position angles is large. Here we are looking along rather than across the mean direction of the magnetic field. Linear-polarization data for table 2 were calculated from observations of 29 stars in the V passband by Serkowski (1965). No allowance was made for possible correlations between closely neighboring stars. Although $|\theta_i|$ is not much larger than for h and χ Persei, $\sigma_{V/I}$ is much larger because the dispersions $\sigma_{Q/I}$ and $\sigma_{U/I}$ are so great. Because of the large disorientation, D is considerably less than 1. In order that the model be reliable ($n \gg 1$) we must assume that the dispersion in the polarization p_i of the slabs is large. We also note that σ_θ and $|\theta_i|$ are about the same size.

Despite the probable shortcomings of the model we can make a reasonable prediction $\sigma_{V/I} \simeq 10^{-4}$ for this cluster. In view of the predicted wavelength dependence of V/I (see figs. 6 and 7) and the high reddening in this cluster, observations near 1 μ would likely to the most fruitful.

This example, VI Cygni, is not the only possibility for circular-polarization observations, as shown by an interesting diagram in Verschuur (1970). For many clusters, $\langle Q/I \rangle$ and σ_θ are plotted as a function of galactic longitude. There are several clusters for which

TABLE 2

AVERAGE POLARIZATION PARAMETERS FOR TWO CLUSTERS

	OBSERVED					DERIVED			
CLUSTER	$\langle Q/I \rangle$	$\sigma_{Q/I}$	$\sigma_{U/I}/\sigma_{Q/I}$	σ_θ	D	$|\theta_i|$	$\sigma_{V/I}/(\langle \Delta e_i^2 \rangle/\langle p_i^2 \rangle)^{1/2}$	n	σ_θ
h and χ Persei, 135°, −4°....	3.6×10^{-2}	4.3×10^{-3}	1.	4°	1	22°	9×10^{-5}	≥ 70	2°7
VI Cygni, 80°, +1°.....	1.3×10^{-2}	2.3×10^{-2}	1.2	39°	≤ 0.33	26°	7×10^{-4}	≥ 0.3	...

TABLE 3

MEASUREMENTS OF CIRCULAR POLARIZATION FOR NINE STARS

NAME	HD	V	E_{B-V}	$10^2(P/I)_V$	θ_V	$\theta(0.33\,\mu) - \theta(0.94\,\mu)$	D	$10^4 V/I^*$	
								Red-infrared	Blue
+56°718	17378	6.26	0.97	4.56	121	...	0.52	+1.13 ± 0.30	−1.76 ± 0.55
BS 1040	21389	4.55	0.55	3.66	121	3	0.74	−0.33 ± 0.45	−0.66 ± 0.21
+56°824	22253	6.53	0.60	1.86	122	−16	0.35	−0.82 ± 0.43	+0.66 ± 0.27
+52°714	23675	6.70	0.70	2.94	130	...	0.47	...	−0.85 ± 0.36
+52°726	24431	6.73	0.67	2.09	118	−15	0.35	+0.15 ± 0.43	−1.05 ± 0.32
χ Aur	36371	4.77	0.44	2.19	176	− 9	0.56	+0.86 ± 0.26†	−0.67 ± 0.17
9 Gem	43384	6.25	0.58	2.96	169	...	0.56	−0.84 ± 0.30	...
o Sco	147084	4.57	0.74	4.09	32	...	0.62	+1.92 ± 0.28†	...
+18°4085	183143	6.86	1.27	6.17	179	...	0.42	+1.50 ± 0.39	...

* Passbands 7150–8700 Å and 3300–4700 Å, except 7800–8700 Å (where indicated by dagger).

both $\langle Q/I \rangle$ and σ_θ are large. These should have measureable circular polarization.

V. OBSERVATIONS

Finally, what observations are feasible in the near future? In table 3 we report the results of recent observations of interstellar circular polarization made at the 36-inch (92-cm) telescope of McDonald Observatory on the nights of 1973 February 12–17, using a new version of the pockels cell type[2] polarimeter with RCA C31034A photomultiplier tubes, under the control of a "Nova" minicomputer. Observations made with the instrument at eight position angles spaced at 45° were averaged to eliminate the effects of the system's spurious response to linear polarization. The errors listed are 1 σ based on photon statistics and do not allow for any systematic errors which at the present are difficult to estimate. We note though that there is no dependence of the observed circular polarization on the position angle of linear polarization, and that for the one star in common with the six previously detected by Kemp and Wolstencroft (1972), o Sco, our result agrees well with an extrapolation of their values towards the infrared (fig. 7).

In the above observations, the counting rate was about 0.8 MHz with a 1500 Å passband for a 6th magnitude star. For this example, detection of circular polarization of order 10^{-4} at the 3 σ level requires an integration time of about 20 minutes. We can then calculate that 10th magnitude stars could be measured readily with a 200-cm telescope. Stars brighter than 5th magnitude are not necessarily measured correspondingly faster because of the extreme counting rates required.

A number of criteria might be considered together in selecting stars to observe. Significant interstellar absorption and linear polarization are obviously important indicators, but in the limited observations so far there is only a slight tendency for V/I to increase with either E_{B-V} or p_V. A low ratio of polarization to

[2] e.g., Angel and Landstreet 1970.

extinction might indicate changing alignment; for the stars in table 3, $D < 0.74$. It is not surprising that no strong correlations have appeared because of the dependence of V/I on the additional geometrical factor of changing alignment which must vary markedly throughout the Galaxy. Stars in regions with a high dispersion in position angle should be systematically more strongly circularly polarized.

An interesting subset of stars which might be circularly polarized are those for which the position angle of linear polarization is wavelength dependent. Following a discussion at IAU Colloquium No. 23 (Tucson, 1972 November) G. Coyne has circulated a list of 27 stars with definite $\Delta\theta$. Of these, 13 are noted to have some intrinsic polarization, so that changing grain alignment is not necessarily the cause of $\Delta\theta$. Although these stars may show circular polarization they will not necessarily give the maximum desired information because of the uncertain contribution of the intrinsic component. Two circularly polarized stars which might fall in this class are HD 169454 (Kemp and Wolstencroft 1972) and NU Orionis (J. R. P. Angel, private communication). Of the remaining 14, σ Sco has been measured previously, χ Aur and possibly HD 22253 are new detections, in the blue and red, and BS 1040 and HD 24431 are polarized in the blue (table 3). The other nine have not been observed yet.

Although a broad blue passband is a good possibility for an extended search, the near-infrared, at about 1 μ, seems to hold the most promise since the predicted circular polarization is relatively large (figs. 6, 7) and highly reddened stars may be observed more easily because of the reduced interstellar extinction. This choice may be particularly important in observing clusters of stars.

In summary, it appears possible that an abundance of observational material could be obtained. Such data would be desirable, since when subjected to the type of analysis suggested above they reveal important new details of the nature of the interstellar grains and the structure of the galactic magnetic field.

I would like to thank the Director of McDonald Observatory for making telescope time available, G. V. Coyne, S.J. for providing a list of stars with wavelength-dependent position angles, and Dr. J. R. P. Angel for the use of his polarimeter. This work is supported by the National Research Council of Canada.

APPENDIX

This particular outline of the derivation of the transfer equations for the Stokes parameters follows Serkowski (1962), whose equations are referred to with the prefix S. Serkowski's treatment is based on the discussion by van de Hulst (1957).

In the interstellar medium there is neither circular birefringence nor circular dichroism present so that the complex amplitudes E_j of the electric vector along axes 1 and 2 of the mean grain profile (see fig. 1) are changed according to the simple relation (cf. eqs. [S12]–[S15])

$$\begin{pmatrix} E_2 \\ E_1 \end{pmatrix}' = \begin{pmatrix} A_2 & 0 \\ 0 & A_1 \end{pmatrix} \begin{pmatrix} E_2 \\ E_1 \end{pmatrix} . \qquad (A1)$$

The complex optical constants A_j describing a slice of the medium of thickness ds are related to the formal refractive indices of the medium,

$$m_j = 1 + (\epsilon_j - i\sigma_j)\lambda/2\pi \qquad (A2)$$

by

$$A_j = 1 - ds(\sigma_j + i\epsilon_j) . \qquad (A3)$$

Clearly ϵ_j is the phase change (retardation) per unit pathlength and σ_j is half the linear extinction coefficient. The relationship of the m_j to the grain parameters is reviewed in § IIb.

Thus from the definitions of I, Q, U, V (vector C)[3] the transformation matrix F in

$$C' = FC \qquad (A4)$$

can be calculated. Using equation (S16) we have

$$F = \begin{pmatrix} 1 & 0 & 0 & 0 \\ 0 & 1 & 0 & 0 \\ 0 & 0 & 1 & 0 \\ 0 & 0 & 0 & 1 \end{pmatrix} + ds \begin{pmatrix} -\delta & \Delta\sigma & 0 & 0 \\ \Delta\sigma & -\delta & 0 & 0 \\ 0 & 0 & -\delta & -\Delta\epsilon \\ 0 & 0 & \Delta\epsilon & -\delta \end{pmatrix} , \qquad (A5)$$

where for conciseness we have used[4] $\delta = \sigma_1 + \sigma_2$, $\Delta\sigma = \sigma_1 - \sigma_2$, and $\Delta\epsilon = \epsilon_1 - \epsilon_2$. If the matrix on the right is denoted H, then clearly

$$\frac{dC}{ds} = HC , \qquad (A6)$$

[3] Here the Stokes parameters are defined in a coordinate system fixed to the mean grain profile. Linear polarization along axis 2 is positive Q, whereas positive U lies at position angle (counterclockwise) 45° relative to axis 2. Positive V is a counterclockwise rotation.

[4] This can be generalized to include the effects of spherical or nonaligned particles. Only the extinction changes; δ becomes $\sigma_1 + \sigma_2 + 2\sigma_s$ and $\Delta\sigma$ and $\Delta\epsilon$ remain the same.

and alternatively

$$I^{-1}dI/ds = -\delta + \Delta\sigma Q/I , \qquad (A7)$$

$$d(Q/I)/ds = \Delta\sigma - \Delta\sigma(Q/I)^2 , \qquad (A8)$$

$$d(U/I)/ds = -\Delta\epsilon V/I - \Delta\sigma(Q/I)(U/I) , \qquad (A9)$$

$$d(V/I)/ds = \Delta\epsilon U/I - \Delta\sigma(Q/I)(V/I) . \qquad (A10)$$

Equations (8) and (9) given by Martin (1972) corresponding to (A9) and (A10), each contain one wrong sign, but the terms involved were not actually used in the analysis because of their small size. These erroneous signs repeat those found in Serkowski's equations (S103) and (S104).

Up to this point the polarization has been described with reference to a coordinate system fixed to the mean grain profile. The transformation of the Stokes parameters to a more general (sky) coordinate system rotated clockwise by an angle ψ relative to the grain system (see, i.e., fig. 1) is

$$C_{\text{sky}} = RC_{\text{grain}} , \qquad (A11)$$

where

$$R = \begin{pmatrix} 1 & 0 & 0 & 0 \\ 0 & \cos 2\psi & -\sin 2\psi & 0 \\ 0 & \sin 2\psi & \cos 2\psi & 0 \\ 0 & 0 & 0 & 1 \end{pmatrix} . \qquad (A12)$$

Parameters I and V are invariant under rotation. From equations (A4) and (A5) we find

$$dC_{\text{sky}}/ds = RH_{\text{grain}}R^{-1}C_{\text{sky}}$$

$$= H_{\text{sky}}C_{\text{sky}} , \qquad (A13)$$

where

$$H_{\text{sky}} =$$

$$\begin{pmatrix} -\delta & \Delta\sigma\cos 2\psi & \Delta\sigma\sin 2\psi & 0 \\ \Delta\sigma\cos 2\psi & -\delta & 0 & \Delta\epsilon\sin 2\psi \\ \Delta\sigma\sin 2\psi & 0 & -\delta & -\Delta\epsilon\cos 2\psi \\ 0 & -\Delta\epsilon\sin 2\psi & \Delta\epsilon\cos 2\psi & -\delta \end{pmatrix} . \qquad (A14)$$

Equation (A14) can also be reached by introducing the rotation in equation (A1).

Interstellar polarization is usually quite weak so that

$$\frac{\Delta\sigma}{\delta} \, Q/I \ll 1 \, , \quad (Q/I)^2 \ll 1 \, , \quad (U/I)^2 \ll 1 \, ,$$

$$(Q/I)(U/I) \ll 1 \, , \quad \text{and} \quad V/I \ll 1 \, . \quad \text{(A15)}$$

Important simplifications can be made in the transfer equations by dropping many negligible terms. This turns out to be equivalent to setting the elements in matrix H or H_{sky} that are above the diagonal equal to zero. With this approximation equation (A13) leads to equations (1)–(4) which are used throughout this paper.

REFERENCES

Angel, J. R. P., and Landstreet, J. D. 1970, *Ap. J. (Letters)*, **160**, L147.
Carrasco, L., Strom, S. E., and Strom, K. M. 1973, *Ap. J.*, **182**, 95.
Coyne, G. V. 1973, in *Planets, Stars, and Nebulae, studied with Photopolarimetry*, ed. T. Gehrels (Tucson: University of Arizona Press).
Coyne, G. V., and Gehrels, T. 1966, *A.J.*, **71**, 355.
Garrison, R. F. 1967, *Ap. J.*, **147**, 1003.
Gehrels, T., and Silvester, A. B. 1965, *A.J.*, **70**, 579.
Greenberg, J. M. 1968, in *Stars and Stellar Systems*, Vol. **7**, ed. L. H. Aller and B. M. Middlehurst (Chicago: University of Chicago Press), p. 221.
Kemp, J. C. 1972, *Ap. J. (Letters)*, **175**, L37.
Kemp, J. C., and Wolstencroft, R. D. 1972, *Ap. J. (Letters)*, **176**, L115.
Lind, A. C., and Greenberg, J. M. 1966, *J. Appl. Phys.*, **37**, 3195.
Martin, P. G. 1971, *M.N.R.A.S.*, **153**, 279.
———. 1972, *ibid.*, **159**, 179.
———. 1973, in *Planets, Stars, and Nebulae, studied with Photopolarimetry*, ed. T. Gehrels (Tucson: University of Arizona Press).
Martin, P. G., Illing, R. M. E., and Angel, J. R. P. 1972, *M.N.R.A.S.*, **159**, 191.
Mathewson, D. S., and Ford, V. L. 1970, *Mem. R.A.S.*, **74**, 139.
Schmidt, Th. 1958, *Zs. f. Ap.*, **46**, 145.
Serkowski, K. 1962, *Adv. Astr. and Ap.*, **1**, 289.
———. 1965, *Ap. J.*, **141**, 1340.
———. 1968, *ibid.*, **154**, 115.
———. 1971, *Proc. IAU Coll. No. 15*, Veröff. Remeis-Sternwarte Bamberg, Bd. 9, No. 100, p. 11.
———. 1973, in *Interstellar Grains and Molecules*, ed. J. M. Greenberg and H. C. van de Hulst (Dordrecht: Reidel).
Spitzer, L., Jr. 1968, *Diffuse Matter in Space* (New York: Wiley).
Treanor, P. J. 1963, *A.J.*, **68**, 185.
van de Hulst, H. C. 1957, *Light Scattering by Small Particles* (New York: Wiley).
Verschuur, G. L. 1970, in *Interstellar Gas Dynamics*, ed. H. J. Habing (Dordrecht: Reidel), p. 150.